1 **Flexpart v10.1 simulation of source contributions to Arctic black carbon**

3 Chunmao Zhu[1], Yugo Kanaya[1,2], Masayuki Takigawa[1,2], Kohei Ikeda[3], Hiroshi Tanimoto[3],

4 Fumikazu Taketani[1,2], Takuma Miyakawa[1,2], Hideki Kobayashi[1,2], Ignacio Pisso[4]

6 [1]Research Institute for Global Change, Japan Agency for Marine–Earth Science and

7 Technology (JAMSTEC), Yokohama 2360001, Japan

8 [2]Institute of Arctic Climate and Environmental Research, Japan Agency for Marine–Earth

9 Science and Technology, Yokohama 2360001, Japan

10 [3]National Institute for Environmental Studies, Tsukuba 305-8506, Japan

11 [4]NILU – Norwegian Institute for Air Research, Kjeller 2027, Norway

13 Correspondence to Chunmao Zhu (chmzhu@jamstec.go.jp)

14   **Abstract**

15   The Arctic environment is undergoing rapid changes such as faster warming than the

16   global average and exceptional melting of glaciers in Greenland. Black carbon (BC) particles,

17   which are a short-lived climate pollutant, are one cause of Arctic warming and glacier

18   melting. However, the sources of BC particles are still uncertain. We simulated the potential

19   emission sensitivity of atmospheric BC present over the Arctic (north of 66° N) using the

20   Flexpart Lagrangian transport model (version 10.1). This version includes a new aerosol wet

21   removal scheme, which better represents particle-scavenging processes than older versions

22   did. Arctic BC at the surface (0–500 m) and high altitudes (4750–5250 m) is sensitive to

23   emissions in high latitude (north of 60° N) and mid-latitude (30–60° N) regions, respectively.

24   Geospatial sources of Arctic BC were quantified, with a focus on emissions from

25   anthropogenic activities (including domestic biofuel burning) and open biomass burning

26   (including agricultural burning in the open field) in 2010. We found that anthropogenic

27   sources contributed 82 % and 83 % of annual Arctic BC at the surface and high altitudes,

28   respectively. Arctic surface BC comes predominantly from anthropogenic emissions in

29   Russia (56 %), with gas flaring from the Yamalo-Nenets Autonomous Okrug and Komi

30   Republic being the main source (31 % of Arctic surface BC). These results highlight the need

31   for regulations to control BC emissions from gas flaring to mitigate the rapid changes in the

32   Arctic environment. In summer, combined open biomass burning in Siberia, Alaska, and

33   Canada contributes 56–85 % (75 % on average) and 40–72 % (57 %) of Arctic BC at the

34   surface and high altitudes, respectively. A large fraction (40 %) of BC in the Arctic at high

35   altitudes comes from anthropogenic emissions in East Asia, which suggests that the rapidly

36   growing economies of developing countries could have a non-negligible effect on the Arctic.

37   To our knowledge, this is the first year-round evaluation of Arctic BC sources that has been

38   performed using the new wet deposition scheme in Flexpart. The study provides a scientific

39   basis for actions to mitigate the rapidly changing Arctic environment.

41 **1   Introduction**

42   The Arctic region has experienced warming at a rate twice that of the global average in

43   recent decades (Cohen et al., 2014). The Arctic cryosphere has been undergoing

44   unprecedented changes since the mid-1800s (Trusel et al., 2018). Glacier cover in Greenland

45   reached its historically lowest level in summer 2012 (Tilling et al., 2015). Evidence indicates

46   that the emissions and transport of greenhouse gases and aerosols to the Arctic region are

47   contributing to such warming and melting of snow and ice (Keegan et al., 2014; Najafi et al.,

48   2015). Short-lived climate pollutants such as black carbon (BC) particles (e.g., Sand et al.,

49   2016; Yang et al., 2019), sulfate aerosol (Yang et al., 2018), tropospheric ozone, and

50   methane greatly affect the Arctic climate (AMAP, 2015; Quinn et al., 2008).

51   BC particles are emitted during incomplete combustion of fossil fuels, biofuels, and

52   biomass. BC warms the atmosphere by direct absorption of solar radiation. The deposition

53   of BC on snow and ice surfaces accelerates their melting through decreasing albedo, which

54   contributes to the rapid loss of glaciers. In the Arctic region, ground-based observations

55   have indicated that BC shows clear seasonal variations, with elevated mass concentrations

56   in winter and spring (the so-called Arctic haze) and low values in summer (Law and Stohl,

57   2007). Such seasonal variations are explained by increased transport from lower latitudes in

58   the cold season and increased wet scavenging in the warm season (Shaw, 1995; Garrett et

59   al., 2011; Shen et al., 2017).

60   The presence of BC particles in the Arctic is mainly attributed to emissions in high-latitude

61   regions outside the Arctic, such as northern Europe and Russia (Stohl, 2006; Brock et al.,

62   2011). This is partly caused by the polar dome (Stohl, 2006), which is formed because of the

63   presence of constant potential temperature near the surface. The emissions in high-latitude

64   regions are transported to the Arctic region and trapped in the dome, which increases the

65   surface concentration. Recently, Schmale et al. (2018) suggested that local emissions from

66   within the Arctic are another important source, and these are expected to increase in the

67   future.

68   Although numerous studies have been performed, results regarding regional

69   contributions of BC sources in the Arctic are still inconclusive. For example, ground-based

70   observations and Lagrangian transport model results reported by Winiger et al. (2016)

71   showed that BC in Arctic Scandinavia is predominantly linked to emissions in Europe. Over

72   the whole Arctic region (north of 66° N), Russia contributes 62 % to surface BC in terms of

73   the annual mean (Ikeda et al., 2017). Gas flaring in Russia has been identified as a major

74   (42 %) source of BC at the Arctic surface (Stohl et al., 2013). Xu et al. (2017) found that

75   anthropogenic emissions from northern Asia contribute 40–45 % of Arctic surface BC in

76   winter and spring. However, the results of some other studies have suggested that Russia,

77   Europe, and South Asia each contribute 20–25 % of BC to the low-altitude springtime Arctic

78   haze (Koch and Hansen, 2005). Sand et al. (2016) found that the surface temperature in the

79   Arctic is most sensitive to emissions in Arctic countries, and Asian countries contribute

80   greatly to Arctic warming because of the large absolute amount of emissions. With these

81   large disagreements among studies, it is thus necessary to unveil BC sources in the Arctic

82   with high precision simulations.

83   Various models have been used to investigate BC sources in the Arctic. Depending on the

84   simulation method, these models are generally categorized as Lagrangian transport models

85   (Hirdman et al., 2010; Liu et al., 2015; Stohl et al., 2006, 2013), chemical transport models

86   (Ikeda et al., 2017; Koch and Hansen, 2005; Qi et al., 2017; Shindell et al., 2008; Wang et al.,

87   2011; Xu et al., 2017), and global climate models (Ma et al., 2013; Schacht et al., 2019; H.

88   Wang et al., 2014) (Table 1). The treatment of wet-scavenging parameterizations is a key

89 factor affecting the model performance, which determines the uncertainties related to BC

90 particle removal (Kipling et al., 2013; Schacht et al., 2019; Q. Wang et al., 2014). The use of

91 emission inventories is another important factor that affects the simulation results (Dong et

92 al., 2019). The observations of BC that are used for model comparisons may be biased by a

93 factor of 2 depending on the method used (Sinha et al., 2017; Sharma et al., 2017). There

94 are still large uncertainties regarding the sources of BC in the Arctic with respect to emission

95 sectors (anthropogenic sources and open biomass burning) and geospatial contributions

96 (Eckhardt et al., 2015).

97   The FLEXible PARTicle dispersion model (Flexpart) had been used to investigate the

98 transport pathways and source contributions of BC in the Arctic (Stohl et al., 1998, 2006,

99 2013). Of Flexpart model up to version 9, wet removal was treated considering below-cloud

100 and within-cloud scavenging processes (Hertel et al., 1995; McMahon and Denison, 1979),

101 which depends on cloud liquid water content, precipitation rate and the depth of the cloud.

102 However, clouds were parameterized based on relative humidity, clouds frequently

103 extended to the surface and at times no clouds could be found in grid cells, with unrealistic

104 precipitation (Grythe et al., 2017). Recently, version 10 of Flexpart had been developed in

105 which cloud is differentiated into liquid, solid, and mixed phase, the cloud distribution is

106 more consistent with the precipitation data (Grythe et al., 2017). This improvement in the

107 cloud distribution and phase leads to a more realistic distribution of below-cloud and in-

108 cloud scavenging events. In this study, we quantified region-separated sources of BC in the

109 Arctic in 2010 by using Flexpart v10.1. We first evaluated the model performance by

110 comparing the results with those based on observations at surface sites. The source

111 contributions of emission sectors and geospatial contributions were evaluated by

112 incorporating the Arctic BC footprint into the emission inventories.

2   Materials and methods

2.1 Transport model

The Flexpart model (version 10.1) was run in backward mode to simulate BC footprints in

the Arctic region. The calculation of wet deposition was improved compared with those in

previous versions because in-cloud scavenging and below-cloud scavenging of particles were

separately calculated (Grythe et al., 2017). In previous versions of Flexpart, in the in-cloud

scavenging scheme, the aerosol scavenging coefficient depended on the cloud water

content, which was calculated according to an empirical relationship with precipitation rate,

in which all aerosols had the same nucleation efficiency (Hertel et al., 1995 ; Stohl et al.,

2005). In the new version, the in-cloud scavenging scheme depends on the cloud water

phase (liquid, ice, or mixed phase). Aerosols were set as ice nuclei for ice clouds and as

cloud condensation nuclei for liquid-water clouds, respectively. For mixed-phase clouds, it

was assumed that 10 % of aerosols are ice nuclei and 90 % are cloud condensation nuclei,

because BC is much more efficiently removed in liquid water clouds than in ice clouds (Cozic

et al., 2007; Grythe et al., 2017). The below-cloud scavenging scheme can parameterize

below-cloud removal as a function of aerosol particle size, and precipitation type (snow or

rain) and intensity. The biases produced in simulations using the new scheme are therefore

smaller than those in the old scheme for wet deposition of aerosols, especially at high

latitudes (Grythe et al., 2017).

The Arctic region is defined as areas north of 66° N. The potential BC emission

sensitivities at two heights in the Arctic region, i.e., the surface (0–500 m) and high altitudes

(4750–5250 m), were simulated. The Flexpart outputs were set as gridded retention times.

We performed tests at 500, 2000, and 5000 m, and chose 500 m as the upper boundary

height of the model output. The model was driven with operational analytical data from the

137   European Centre for Medium-Range Weather Forecasts (ECMWF) at a spatial resolution of

138   1° × 1° with 61 vertical levels. Temporally, ECMWF has a resolution of 3 h, with 6 h analysis

139   and 3 h forecast time steps. The simulation period was set at 60 days backward starting

140   from each month in 2010. The maximum lifetime of BC was set at 20 days because its

141   suspension time in the upper atmosphere during long-range transport is longer than that at

142   the surface level (Stohl et al., 2013). We implemented the wet deposition scheme in the

143   backward calculations, but it was not represented in the default setting (Flexpart v10.1,

144   https://www.flexpart.eu/downloads, obtained 10 April 2017).

145   The chemistry and microphysics could not be resolved by Flexpart. The model therefore

146   ignores hydrophobic to hydrophilic state changes and size changes of BC, and assumes that

147   all BC particles are aged hydrophilic particles. This may lead to an overestimation of BC

148   removal and hence force underestimation of simulated BC concentration, especially of fossil

149   fuel combustion sources where BC could be in the hydrophobic state for a few days. A

150   logarithmic size distribution of BC with a mean diameter of 0.16 μm and a standard

151   deviation of 1.96, in accordance with our ship observations in the Arctic, was used (Taketani

152   et al., 2016). The particle density was assumed to be 2000 kg m^{-3}, and 1 million

153   computational particles were randomly generated in the Arctic region for the backward

154   runs.

155   Four ground-based observations made during the period 2007–2011 were used to

156   validate the model performance. The potential BC emission sensitivity at 0–500 m above

157   ground level from a 0.1° grid centered at each site was simulated. Other model

158   parameterizations were consistent with those for the Arctic region, except that 200 000

159   computational particles were released.

160   2.2 Emission inventories

161   We focused on BC sources from anthropogenic emissions and open biomass burning. The

162   Hemispheric Transport of Air Pollution version 2 inventory (HTAP2) for 2010 was used for

163   monthly anthropogenic BC emissions (Janssens-Maenhout et al., 2015), which include

164   sectors from energy, industry, residential and transport. It is worth noting that the

165   residential sector includes not only combustions of fossil fuels, but also biofuels. However,

166   as it has been reported that BC emissions in Russia were underestimated in HTAP2, we used

167   the BC emissions reported by Huang et al. (2015) for Russia, in which the annual BC

168   emissions were 224 Gg yr^{-1}. For open biomass burning, we used the monthly BC emissions

169   from the Global Fire Emissions Database version 3 inventory (GFED3) (van der Werf et al.,

170   2010) for the purposes of intercomparison with other studies, as this version is widely used.

171   The term "open biomass burning" here indicates burning of biomass in the open field as is

172   determined by the remote sensing measurement basis, including forest, agricultural waste,

173   peat fires, grassland and savanna, woodland, deforestation and degradation, where biofuel

174   burning for residential use is not included. Geospatial distributions of emissions from

175   anthropogenic sources and open biomass burning in January and July are shown in Fig. S1.

176   2.3 Calculation of Arctic BC source contributions

177   The source contributions to Arctic BC were derived by incorporating the gridded

178   retention time into the column emission flux, which was derived from the emission

179   inventories in each grid. Calculations for anthropogenic sources and open biomass burning

180   were performed separately and the sum was used. For anthropogenic sources, the regions

181   were separated into North America and Canada (25–80° N, 50–170° W), Europe (30–80° N,

182   0–30° E), Russia (53–80° N, 30–180° E), East Asia (35–53° N, 75–150° E and 20–35° N, 100–

183   150° E), and others (the rest) (Fig. 1a). For open biomass burning sources, the regions were

184   separated into Alaska and Canada (50–75° N, 50–170° W), Siberia (50–75° N, 60–180° E),

185   and others (Fig. 1b).

186   2.3 Observations

187   BC levels simulated by Flexpart were compared with those based on surface observations

188   at four sites: Barrow, USA (156.6° W, 71.3° N, 11 m asl), Alert, Canada (62.3° W, 82.5° N,

189   210 m asl), Zeppelin, Norway (11.9° E, 78.9° N, 478 m asl), and Tiksi, Russia (128.9° E, 71.6°

190   N, 8 m asl). Aerosol light absorption was determined by using particle soot absorption

191   photometers (PSAPs) at Barrow, Alert, and Zeppelin, and an aethalometer at Tiksi. For PSAP

192   measurements, the equivalent BC values were derived using a mass absorption efficiency of

193   10 $m^2 g^{-1}$. The equivalent BC at Tiksi, which was determined with an aethalometer, was

194   obtained directly. These measurement data were obtained from the European Monitoring

195   and Evaluation Programme and World Data Centre for Aerosols database

196   (http://ebas.nilu.no) (Tørseth et al., 2012).

197   It is worth noting that uncertainties could be introduced by using different BC

198   measurement techniques. An evaluation of three methods for measuring BC at Alert,

199   Canada indicated that an average of the refractory BC determined with a single-particle soot

200   photometer (SP2) and elemental carbon (EC) determined from filter samples give the best

201   estimate of BC mass (Sharma et al., 2017). Xu et al. (2017) reported that the equivalent BC

202   determined with a PSAP was close to the average of the values for refractory BC and EC at

203   Alert. In this study, we consider that the equivalent BC values determined with a PSAP at

204   Barrow, Alert, and Zeppelin to be the best estimate. There may be uncertainties in the

205   equivalent BC observations performed with an aethalometer at Tiksi because of co-existing

206   particles such as light-absorptive organic aerosols, scattering particles, and dusts

207   (Kirchstetter et al., 2004; Lack and Langridge, 2013). Interference by the filter and

208 uncertainties in the mass absorption cross section could also contribute to the bias

209 observed in measurements made with an aethalometer at Tiksi.

210 **3   Results and discussion**

211 **3.1. Comparisons of simulations with BC observations at Arctic surface sites**

212   Flexpart generally reproduced the seasonal variations in BC at four Arctic sites well

213 [Pearson correlation coefficient (R) = 0.53–0.80, root-mean-square error (RMSE) = 15.1–56.8

214 ng m^{-3}] (Fig. 2). Winter maxima were observed for the four sites, while a secondary

215 elevation was observed for Alert and Tiksi. At Barrow, the observed high values of BC were

216 unintentionally excluded during data screening in the forest fire season in summer (Stohl et

217 al., 2013); the original observed BC is supposed to be higher as was reflected by the

218 simulation. This seasonality is probably related to relatively stronger transport to the Arctic

219 region in winter, accompanied by lower BC aging and inefficient removal, as simulated by

220 older versions of Flexpart (Eckhardt et al., 2015; Stohl et al., 2013).

221   From January to May at Barrow and Alert, the mean BC simulated by Flexpart v10.1 were

222 32.2 ng m^{-3} and 31.2 ng m^{-3}, respectively. Which was 46 % lower than the observations

223 (59.3 ng m^{-3} and 58.2 ng m^{-3}, respectively). This is probably related to the inadequate BC

224 emission in the inventory, although seasonal variations in residential heating are included in

225 HTAP2, which would reduce the simulation bias (Xu et al., 2017). Simulations by GEOS-Chem

226 using the same emission inventories also underestimated BC levels at Barrow and Alert

227 (Ikeda et al., 2017; Xu et al., 2017). The underestimation by Flexpart could also be partly

228 contributed by the assumption that all particles are hydrophilic, where the BC scavenging

229 could be overestimated. The corresponding uncertainties are larger in winter months, when

230 there are more sources from fossil fuel combustion.

231   At Zeppelin, the Flexpart-simulated BC (39.1 ng m^{-3} for annual mean) was 85 % higher

232   than the observed value (21.1 ng m^{-3} for annual mean), especially in winter (112% higher). It

233   has been reported that riming in mixed-phase clouds occurs frequently at Zeppelin (Qi et al.,

234   2017). During the riming process, BC particles act as ice particles and collide with the

235   relatively numerous water drops, which form frozen cloud droplets, and then snow is

236   precipitated. This results in relatively efficient BC scavenging (Hegg et al., 2011). Such a

237   process could not be dealt with by the model. At Tiksi, Flexpart underestimated BC (74.4 ng

238   m^{-3} for annual mean) in comparison with observation (104.2 ng m^{-3} for annual mean). Other

239   than the hydrophilic BC assumption and underestimated BC emission in the simulation as

240   the cases for Barrow and Alert, the observations at Tiksi by an aethalometer could

241   containing light-absorbing particles other than BC, resulting in higher observed

242   concentrations if compared with those obtained by SP2, EC and PSAP.

243   Anthropogenic emissions are the main sources of BC at the four Arctic sites from late

244   autumn to spring, whereas open biomass burning emissions make large contributions in

245   summer. From October to April, anthropogenic emissions accounted for 87–100 % of BC

246   sources at all the observation sites. At Barrow, open biomass burning accounted for 35–

247   78 % of BC in June–September (Fig. 2). There are large interannual variations in both

248   observed and simulated BC (Fig. S2). In June–August 2010, the mean contributions of open

249   biomass burning to BC were 6.3, 2.4, and 8.6 times those from anthropogenic sources at

250   Alert, Zeppelin, and Tiksi, respectively. In this study, we focused on BC in the Arctic region in

251   2010.

252   **3.2 Potential emission sensitivity of Arctic BC**

253   The potential emission sensitivities (footprint) of Arctic BC showed different patterns

254   with respect to altitude. The Arctic surface is sensitive to emissions at high latitudes (>60°

255   N). Air masses stayed for over 60 s in each of the 1° grids from the eastern part of northern

256   Eurasia and the Arctic Ocean before being transported to the Arctic surface in the winter,

257   represented by January (Fig. 3a). In comparison, during the summer, represented by July, BC

258   at the Arctic surface was mainly affected by air masses that originated from the Arctic

259   Ocean and the Norwegian Sea (Fig. 3b). These results imply that local BC emissions within

260   the Arctic regions, although relatively weak compared with those from the mid-latitude

261   regions, could strongly affect Arctic air pollution. Local BC emissions are important in the

262   wintertime because the relatively stable boundary layer does not favor pollution dispersion.

263   Recent increases in anthropogenic emissions in the Arctic region, which have been caused

264   by the petroleum industry and development of the Northern Sea Route, are expected to

265   cause deterioration of air quality in the Arctic. Socio-economic developments in the Arctic

266   region would increase local BC emissions, and this will be a non-negligible issue in the future

267   (Roiger et al., 2015; Schmale et al., 2018).

268   BC at high altitudes in the Arctic is more sensitive to mid-latitude (30–60° N) emissions,

269   especially in wintertime. In January, air masses hovered over the Bering Sea and the North

270   Atlantic Ocean before arriving at the Arctic (Fig. 3c). A notable corridor at 30–50° N covering

271   Eurasia and the United States was the sensitive region that affected BC at high altitudes in

272   the Arctic in January. These results indicate that mid-latitude emissions, especially those

273   with relatively large strengths from East Asia, East America, and Europe, could alter the

274   atmospheric constituents at high altitudes in the Arctic. Central to east Siberia was the most

275   sensitive region for BC at high altitudes in the Arctic in July (Fig. 3d). These results suggest

276   that pollutants from frequent and extensive wildfires in Siberia in summer are readily

277   transported to high altitudes in the Arctic. Boreal fires are expected to occur more

278   frequently and over larger burning areas under future warming (Veira et al., 2016),

279   therefore the atmospheric constituents and climate in the Arctic could undergo more rapid

280   changes.

281   **3.3 Seasonal variations and sources of Arctic surface BC**

282   Arctic surface BC showed clear seasonal variations, with a primary peak in winter–spring

283   (December–March, 61.8–82.8 ng m^{-3}) and a secondary peak in summer (July, 52.7 ng m^{-3}).

284   BC levels were relatively low in May–June (21.8–23.1 ng m^{-3}) and September–November

285   (34.1–40.9 ng m^{-3}) (Fig. 4a). This seasonality agrees with observations and simulations at

286   Alert, Tiksi, and Barrow if consider the unintentional data exclusion (Stohl et al., 2013), and

287   previous studies targeting the whole Arctic (Ikeda et al., 2017; Xu et al., 2017). Compared

288   with the study reported by Stohl et al. (2013), the current work using the new scheme

289   produced smaller discrepancies between the simulated data and observations. Although the

290   simulation periods (monthly means for 2007–2011 in this study and for 2008–2010 in the

291   old scheme) and the anthropogenic emission inventories (HTAP2 in this study and ECLIPSE4

292   in the previous study) are different, the new scheme shows potential for better representing

293   BC transport and removal processes in the Arctic.

294   The annual mean Arctic BC at the surface was estimated to be 48.2 ng m^{-3}. From October

295   to April, anthropogenic sources accounted for 96–100 % of total BC at the Arctic surface.

296   Specifically, anthropogenic emissions from Russia accounted for 61–76 % of total BC in

297   October–May (56 % annually), and was the dominant sources of Arctic BC at the surface.

298   From an isentropic perspective, the meteorological conditions in winter favored the

299   transport of pollutants from northern Eurasia to the lower Arctic, along with diabatic cooling

300   and strong inversions (Klonecki et al., 2003). In comparison, open biomass burning from

301   boreal regions accounted for 56–85 % (75 % on average) of Arctic BC at the surface in

302   summer; open biomass burning emissions from North America and Canada accounted for

303 54 % of total Arctic surface BC in June, and those from Siberia accounted for 59–61 % in

304 July–August. Wildfires in the boreal forests in summer had a major effect on air quality in

305 the Arctic.

306  On an annual basis, anthropogenic sources and open biomass burning emissions

307 accounted for 82 % and 18 %, respectively, of total Arctic surface BC. In which, gas flaring

308 and residential burning (including burning of fossil fuels and biofuels) are accounting for

309 36 % (28–57 % in October–March) and 15 % (13–25 % in October–March), respectively (Fig.

310 5a-b). Our results support Stohl et al. (2013) that residential combustion emissions,

311 especially in winter are important sources of Arctic BC (Table 1). We estimated a

312 contribution of gas flaring to Arctic surface BC of 17.5 ng m^{-3} (36% of total). In comparison,

313 the value was estimated as 11.8 ng m^{-3} using an average Arctic surface BC of 28 ng m^{-3} and

314 a fraction from gas flaring of 42 % evaluated by earlier versions of Flexpart (Stohl et al.,

315 2013; Winiger et al., 2019). The different contribution could be partly attributed to the

316 difference in gas flaring emission inventory. BC emission from gas flaring in Russia by Huang

317 et al. (2015) was used in the current study, where total BC emission from gas flaring in

318 Russia in 2010 was ca. 81.1 kilotonne, which was larger than the estimate of ca. 64.9

319 kilotonne by GAINS inventory (Klimont et al., 2017) used by Stohl et al. (2013). Moreover,

320 Adopting ECLIPSEv5 inventory as was used by Winiger et al. (2019), we estimated that gas

321 flaring was contributing 14.4 ng m^{-3} to Arctic surface BC using Flexpart v10.1, a value 22 %

322 higher than those obtained using Flexpart v9. This difference could be attributed to the

323 improvement of the wet-scavenging scheme by Flexpart v10.1.

324  A recent study based on isotope observations at the Arctic sites and Flexpart v9.2

325 simulation suggested that open biomass burning, including open field burning and

326 residential biofuel burning, contributed 39 % of annual BC in 2011–2015 (Winiger et al.,

327   2019) (Table 1). In comparison, we estimated that residential burning and open biomass

328   burning together account for 33 % of total Arctic surface BC. As the residential burning in

329   our study includes burning of both biofuels and fossil fuels, our results indicated that

330   biomass burning has a relatively smaller contribution. Other than the differences in BC

331   removal treatment between different versions of the model, the contribution difference

332   could also be attributed to the different emission inventories and years (2010 versus 2011-

333   2015).

334   The geospatial contributions of anthropogenic sources and open biomass burning

335   emissions can be further illustrated by taking January and July as examples. In January, high

336   levels of anthropogenic emissions from Russia (contributing 64 % of Arctic surface BC),

337   Europe (18 %), and East Asia (9 %) were identified (Fig. 6a). Specifically, Yamalo-Nenets

338   Autonomous Okrug in Russia, which has the largest reserves of Russia's natural gas and oil

339   (Filimonova et al., 2018), was the most notable emission hotspot, which suggests gas-flaring

340   sources. The Komi Republic in Russia was also identified as a strong anthropogenic emitter

341   contributing to Arctic surface BC. These gas-flaring industrial regions in Russia (58–69° N,

342   68–81°E) together contributed 33 % and 31 % of Arctic surface BC for January and the

343   annual mean, respectively. Recently, Dong et al. (2019) evaluated BC emission inventories

344   using GEOS-Chem and proposed that using the inventory compiled by Huang et al. (2015)

345   for Russia, in which gas flaring accounted for 36 % of anthropogenic emissions, had no

346   prominent impact on the simulation performance in Russia and the Arctic. They suggested

347   that use of a new global inventory for BC emissions from natural gas flaring would improve

348   the model performance (Huang and Fu, 2016). These results suggest that inclusion of BC

349   emissions from gas flaring on the global scale is necessary for further BC simulations.

350   In Europe, a relatively high contribution of anthropogenic emissions to Arctic surface BC

351   in January was made by Poland (50–55° N, 15–24° E, contributing 4 % of Arctic surface BC)

352   because of relatively large emission fluxes in the region (Fig. S1a). Anthropogenic emissions

353   from East China, especially those north of ~33° N (33–43° N, 109–126° E), contributed

354   perceptibly (5 %) to Arctic surface BC.

355   In July, contributions from anthropogenic sources shrank to those from Yamalo-Nenets

356   Autonomous Okrug and Komi Republic in Russia, and contributed a lower fraction (3 % of

357   Arctic surface BC) (Fig. 6b). Few open biomass burning sources contributed in January (Fig.

358   6c), but contributions from open biomass burning to Arctic surface BC in July can be clearly

359   seen, mainly from the far east of Russia, Canada, and Alaska (Fig. 6d). Open biomass burning

360   emissions from Kazakhstan, southwest Russia, southern Siberia, and northeast China also

361   contributed to Arctic surface BC, although at relatively low strengths (Fig. 5d and Fig. S1d).

362   However, the contributions from open biomass burning could be higher, as the MODIS

363   burned area, the basis of GFED emission inventories, was underestimated for northern

364   Eurasia by 16 % (Zhu et al., 2017). Evangeliou et al. (2016) estimated a relatively high

365   transport efficiency of BC from open biomass burning emissions to the Arctic, which led to a

366   high contribution, i.e., 60 %, from such sources to BC deposition in the Arctic in 2010. A

367   recent study suggested that open fires burned in western Greenland in summer (31 July to

368   21 August 2017) could potentially alter the Arctic air composition and foster glacier melting

369   (Evangeliou et al., 2019). Although the footprint of Arctic surface BC showed a relatively

370   weak sensitivity to areas such as forests and tundra, in the boreal regions, pollutants from

371   boreal wildfires could have greater effects on the Arctic air composition in summer under

372   future warming scenarios (Veira et al., 2016).

373   **3.4 Sources of Arctic BC at high altitudes**

374   Arctic BC levels at high altitudes showed the highest levels in spring (March–April, 40.5–

375   53.9 ng m^{-3}), followed by those in late autumn to early winter (November–January, 36.5–

376   40.0 ng m^{-3}), and summer (July–August, 33.0–39.0 ng m^{-3}) (Fig. 4c). The annual mean Arctic

377   BC at high altitudes was estimated to be 35.2 ng m^{-3}, which is ca. 73 % of those at the

378   surface. Such a vertical profile is in accordance with those based on aircraft measurements

379   over the High Canadian Arctic (Schulz et al., 2019). Similarly to the case for the surface,

380   anthropogenic sources dominated by residential sectors, transport, industry and energy

381   (excluding gas flaring), accounted for 94–100 % of Arctic BC at high altitudes in October–

382   May (Figs. 4c, 5c). East Asia accounted for 34–65 % of the total BC in October–May (40 %

383   annually). In comparison, using the Community Atmosphere Model version 5 driven by the

384   NASA Modern Era Retrospective-Analysis for Research and Applications reanalysis data and

385   the IPCC AR5 year 2000 BC emission inventory, H. Wang et al. (2014) found that East Asia

386   accounted for 23% of BC burden in the Arctic for 1995–2005. In summer, open biomass

387   burning in the boreal regions accounted for 40–72 % (57 % on average) of Arctic BC at high

388   altitudes, similar to the source contributions to Arctic surface BC. Specifically, open biomass

389   burning sources from Siberia accounted for 40–42 % of Arctic BC at high altitudes in July–

390   August. Annually, anthropogenic sources and open biomass burning accounted for 83 % (in

391   which residential sources accounted for 34%) and 17 %, respectively, of total Arctic BC at

392   high altitudes (Figs. 4d, 5d).

393   Further investigations of geospatial contributions to Arctic BC at high altitudes in January

394   and July provided more details regarding BC sources. In January, the main anthropogenic BC

395   source in East Asia covered a wide range in China (Fig. 7a). Not only east and northeast

396   China, but also southwest China (Sichuan and Guizhou provinces) were the major

397   anthropogenic sources of Arctic BC at high altitudes. In July, anthropogenic sources made a

398 relatively weak contribution to Arctic BC at high altitudes. The regions that were sources of

399 open biomass burning contributions to Arctic BC at high altitudes were mainly the far east of

400 Siberia, Kazakhstan, central Canada, and Alaska, i.e., similar to the sources of Arctic surface

401 BC. Unlike Arctic surface BC, for which the dominant source regions are at high latitudes in

402 both winter and summer, Arctic BC at high altitudes mainly originates from mid-latitude

403 regions (Figs. 6 and 7). In terms of transport pathways, air masses could be uplifted at low-

404 to-mid latitudes and transported to the Arctic (Stohl, 2006). Further investigations are

405 needed to obtain more details of the transport processes.

406 **3.5 Comparison of Flexpart and GEOS-Chem simulations of BC sources**

407 Data for BC sources simulated with Flexpart were compared with those obtained with

408 GEOS-Chem (Ikeda et al., 2017), which is an Eulerian atmospheric transport model, using the

409 same emission inventories. The simulated seasonal variations in Arctic BC levels and source

410 contributions obtained with Flexpart agreed well with those obtained with GEOS-Chem (Fig.

411 S3). The annual mean BC levels at the Arctic surface obtained by Flexpart and GEOS-Chem

412 simulations were 48 and 70 ng m^{-3}, respectively; the high-altitude values simulated by

413 Flexpart and GEOS-Chem were 35 and 38 ng m^{-3}, respectively. The magnitude difference

414 between the BC levels at the Arctic surface could be related to meteorology. ECMWF ERA-

415 Interim data were used as the input for the Flexpart simulation, whereas the GEOS-Chem

416 simulation was driven by assimilated meteorological data from the Goddard Earth

417 Observation System (GEOS-5).

418 The treatments of the BC removal processes could also lead to different simulation

419 results, depending on the model. In terms of BC loss processes, dry and wet depositions

420 were the removal pathways, depending on the particle size and density, in Flexpart. The

421 treatment of meteorology, especially cloud water and precipitation, would therefore affect

422   the uncertainties of the simulations. In Flexpart version 10.1, BC particles are separately

423   parameterized as ice nuclei for ice clouds, cloud condensation nuclei for liquid-water clouds,

424   and 90 % as cloud condensation nuclei for mixed-phase clouds. The separation of mixed-

425   phase clouds is realistic, as 77 % of in-cloud scavenging processes occurred in the mixed

426   phase over a 90 day period starting from December 2006 (Grythe et al., 2017).

427   In GEOS-Chem simulations, the BC aging was parameterized based on the number

428   concentration of OH radicals (Liu et al., 2011). The BC was assumed to be hydrophilic in

429   liquid clouds ($T \geq 258$ K) and hydrophobic when serving as ice nuclei in ice clouds ($T < 258$ K)

430   (Wang et al., 2011), with modifications because the scavenging rate of hydrophobic BC was

431   reduced to 5 % of water-soluble aerosols for liquid clouds (Bourgeois and Bey, 2011). Such a

432   treatment is expected to improve the simulation accuracy (Ikeda et al., 2017).

433   In Lagrangian models, the trajectories of particles are computed by following the

434   movement of air masses with no numerical diffusion, although some artificial numerical

435   errors could be generated from stochastic differential equations (Ramli and Esler, 2016). As

436   a result, long-range transport processes can be well simulated (Stohl, 2006; Stohl et al.,

437   2013). In comparison, Eulerian chemical transport models such as GEOS-Chem have the

438   advantage of simulating non-linear processes on the global scale, which enables treatment

439   of the BC aging processes (coating with soluble components) (Bey et al, 2001; Eastham et

440   al., 2018). However, with GEOS-Chem, the capture of intercontinental pollution plumes is

441   difficult because of numerical plume dissipation (Rastigejev et al., 2010). Nevertheless, the

442   agreement between the Flexpart and GEO-Chem simulations of BC source contributions

443   indicates improved reliability of evaluated source contributions to Arctic BC.

444   **4   Conclusions**

445  The source contributions to Arctic BC were investigated by using a Flexpart (version 10.1)

446 transport model that incorporated emission inventories. Flexpart-simulated BC data agreed

447 well with observations at Arctic sites, i.e., Barrow, Alert, Zeppelin, and Tiksi. The source

448 regions and source sectors of BC at the surface and high altitudes over a wide region in the

449 Arctic north of 66° N were simulated. BC at the Arctic surface was sensitive to local

450 emissions and those from nearby Nordic countries (>60° N). These results emphasize the

451 role of anthropogenic emissions such as gas flaring and development of the Northern Sea

452 Route in affecting air quality and climate change in the Arctic. Anthropogenic emissions in

453 the northern regions of Russia were the main source (56 %) of Arctic surface BC annually. In

454 contrast, BC in the Arctic at high altitudes was sensitive to mid-latitude emissions (30–60°

455 N). Although they are geospatially far from the Arctic, anthropogenic emissions in East Asia

456 made a notable (40 %) contribution to BC in the Arctic at high altitudes annually. Open

457 biomass burning emissions, which were mainly from Siberia, Alaska, and Canada, were

458 important in summer, contributing 56–85 % of BC at the Arctic surface, and 40–72 % at

459 Arctic high altitudes. Future increases in wildfires as a result of global warming could

460 therefore increase the air pollution level during the Arctic summer. This study clarifies the

461 source regions and sectors of BC in the Arctic. This information is fundamental for

462 understanding and tackling air pollution and climate change in the region.

463

464 *Data Availability.* The data set for simulated footprint and BC source contributions is

465 available on request to the corresponding author.

466

467 *Author contributions.* CZ and YK designed the study. CZ, MT, and IP optimized the Flexpart

468 model. CZ performed Flexpart model simulations, conducted analyses, and wrote the

469   manuscript. KI and HT provided data for GEOS-Chem simulations and site observations. All

470   authors made comments that improved the paper.

471

472   *Competing interests.* The authors declare that they have no conflict of interest.

473

474   *Financial Support.* This study was supported by the Environmental Research and Technology

475   Development Fund (2-1505) of the Ministry of the Environment, Japan.

476

477   *Acknowledgment.* We acknowledge staffs from the following university and agencies for BC

478   observational data: Barrow and Tiksi sites are operated by National Oceanic and

479   Atmospheric Administration; Zeppelin site is operated by Stockholm University; and Alert

480   site is operated by Environment and Climate Change Canada. We are grateful to Chandra

481   Mouli Pavuluri (Tianjin University) and an anonymous reviewer for the comments. We thank

482   Helen McPherson, PhD, from Edanz Group (www.edanzediting.com/ac) for editing a draft of

483   this manuscript.

484

485   **References**

486   AMAP Assessment 2015: Black carbon and ozone as Arctic climate forcers, Arctic Monitoring

487   and Assessment Programme (AMAP), Oslo, Norway, 2015.

488   Bey, I., Jacob, D. J., Yantosca, R. M., Logan, J. A., Field, B. D., Fiore, A. M., Li, Q. B., Liu, H. G.

489   Y., Mickley, L. J., and Schultz, M. G.: Global modeling of tropospheric chemistry with

490   assimilated meteorology: Model description and evaluation, J Geophys Res-Atmos, 106,

491   23073-23095, doi:10.1029/2001jd000807, 2001.

492   Bourgeois, Q. and Bey, I.: Pollution transport efficiency toward the Arctic: sensitivity to

493   aerosol scavenging and source regions, J. Geophys. Res., 116, D08213,

494   doi:10.1029/2010JD015096, 2011.

495 Brock, C. A., Cozic, J., Bahreini, R., Froyd, K. D., Middlebrook, A. M., McComiskey, A.,

496 Brioude, J., Cooper, O. R., Stohl, A., Aikin, K. C., de Gouw, J. A., Fahey, D. W., Ferrare, R.

497 A., Gao, R. S., Gore, W., Holloway, J. S., Hubler, G., Jefferson, A., Lack, D. A., Lance, S.,

498 Moore, R. H., Murphy, D. M., Nenes, A., Novelli, P. C., Nowak, J. B., Ogren, J. A., Peischl, J.,

499 Pierce, R. B., Pilewskie, P., Quinn, P. K., Ryerson, T. B., Schmidt, K. S., Schwarz, J. P.,

500 Sodemann, H., Spackman, J. R., Stark, H., Thomson, D. S., Thornberry, T., Veres, P., Watts,

501 L. A., Warneke, C., and Wollny, A. G.: Characteristics, sources, and transport of aerosols

502 measured in spring 2008 during the aerosol, radiation, and cloud processes affecting

503 Arctic Climate (ARCPAC) Project, Atmospheric Chemistry and Physics, 11, 2423-2453,

504 doi:10.5194/acp-11-2423-2011, 2011.

505 Cohen, J., Screen, J. A., Furtado, J. C., Barlow, M., Whittleston, D., Coumou, D., Francis, J.,

506 Dethloff, K., Entekhabi, D., Overland, J., and Jones, J.: Recent Arctic amplification and

507 extreme mid-latitude weather, Nature Geoscience, 7, 627-637, doi:10.1038/Ngeo2234,

508 2014.

509 Cozic, J., Verheggen, B., Mertes, S., Connolly, P., Bower, K., Petzold, A., Baltensperger, U.,

510 and Weingartner, E.: Scavenging of black carbon in mixed phase clouds at the high alpine

511 site Jungfraujoch, Atmos. Chem. Phys., 7, 1797-1807, doi:10.5194/acp-7-1797-2007,

512 2007.

513 Dong, X., Zhu, Q., Fu, J. S., Huang, K., Tan, J., and Tipton, M.: Evaluating recent updated black

514 carbon emissions and revisiting the direct radiative forcing in Arctic, Geophysical

515 Research Letters, 46, 3560– 3570. doi:10.1029/2018GL081242, 2019.

516 Eastham, S. D., Long, M. S., Keller, C. A., Lundgren, E., Yantosca, R. M., Zhuang, J. W., Li, C.,

517 Lee, C. J., Yannetti, M., Auer, B. M., Clune, T. L., Kouatchou, J., Putman, W. M., Thompson,

518 M. A., Trayanov, A. L., Molod, A. M., Martin, R. V., and Jacob, D. J.: GEOS-Chem High

519 Performance (GCHP v11-02c): a next-generation implementation of the GEOS-Chem

520 chemical transport model for massively parallel applications, Geosci Model Dev, 11,

521 2941-2953, doi:10.5194/gmd-11-2941-2018, 2018.

522 Eckhardt, S., Quennehen, B., Olivie, D. J. L., Berntsen, T. K., Cherian, R., Christensen, J. H.,

523 Collins, W., Crepinsek, S., Daskalakis, N., Flanner, M., Herber, A., Heyes, C., Hodnebrog,

524 O., Huang, L., Kanakidou, M., Klimont, Z., Langner, J., Law, K. S., Lund, M. T., Mahmood,

525 R., Massling, A., Myriokefalitakis, S., Nielsen, I. E., Nojgaard, J. K., Quaas, J., Quinn, P. K.,

526 Raut, J. C., Rumbold, S. T., Schulz, M., Sharma, S., Skeie, R. B., Skov, H., Uttal, T., von

527   Salzen, K., and Stohl, A.: Current model capabilities for simulating black carbon and

528   sulfate concentrations in the Arctic atmosphere: a multi-model evaluation using a

529   comprehensive measurement data set, Atmospheric Chemistry and Physics, 15, 9413-

530   9433, doi:10.5194/acp-15-9413-2015, 2015.

531   Evangeliou, N., Balkanski, Y., Hao, W. M., Petkov, A., Silverstein, R. P., Corley, R., Nordgren,

532   B. L., Urbanski, S. P., Eckhardt, S., Stohl, A., Tunved, P., Crepinsek, S., Jefferson, A.,

533   Sharma, S., Nojgaard, J. K., and Skov, H.: Wildfires in northern Eurasia affect the budget of

534   black carbon in the Arctic - a 12-year retrospective synopsis (2002-2013), Atmospheric

535   Chemistry and Physics, 16, 7587-7604, doi:10.5194/acp-16-7587-2016, 2016.

536   Evangeliou, N., Kylling, A., Eckhardt, S., Myroniuk, V., Stebel, K., Paugam, R., Zibtsev, S., and

537   Stohl, A.: Open fires in Greenland in summer 2017: transport, deposition and radiative

538   effects of BC, OC and BrC emissions, Atmospheric Chemistry and Physics, 19, 1393-1411,

539   doi:10.5194/acp-19-1393-2019, 2019.

540   Filimonova, I. V., Komarova, A. V., Eder, L. V., and Provornaya, I. V.: State instruments for the

541   development stimulation of Arctic resources regions, IOP Conference Series: Earth and

542   Environmental Science, 193, 012069, doi:10.1088/1755-1315/193/1/012069, 2018.

543   Garrett, T. J., Brattstrom, S., Sharma, S., Worthy, D. E. J., and Novelli, P.: The role of

544   scavenging in the seasonal transport of black carbon and sulfate to the Arctic,

545   Geophysical Research Letters, 38, L16805, doi:10.1029/2011gl048221, 2011.

546   Grythe, H., Kristiansen, N. I., Zwaaftink, C. D. G., Eckhardt, S., Strom, J., Tunved, P., Krejci, R.,

547   and Stohl, A.: A new aerosol wet removal scheme for the Lagrangian particle model

548   FLEXPART v10, Geosci Model Dev, 10, 1447-1466, doi:10.5194/gmd-10-1447-2017, 2017.

549   Hegg, D. A., Clarke, A. D., Doherty, S. J., and Ström, J.: Measurements of black carbon

550   aerosol washout ratio on Svalbard, Tellus B, 63, 891–900, doi:10.1111/j.1600-

551   0889.2011.00577.x, 2011.

552   Hertel, O., Christensen, J. Runge, E. H., Asman, W. A. H., Berkowicz, R., Hovmand, M. F., and

553   Hov, O.: Development and testing of a new variable scale air pollution model – ACDEP,

554   Atmos. Environ., 29, 1267–1290, 1995.

555   Hirdman, D., Burkhart, J. F., Sodemann, H., Eckhardt, S., Jefferson, A., Quinn, P. K., Sharma,

556   S., Strom, J., and Stohl, A.: Long-term trends of black carbon and sulphate aerosol in the

557   Arctic: changes in atmospheric transport and source region emissions, Atmospheric

558   Chemistry and Physics, 10, 9351-9368, doi:10.5194/acp-10-9351-2010, 2010.

559 Huang, K., and Fu, J. S.: A global gas flaring black carbon emission rate dataset from 1994 to
560   2012, Scientific Data, 3, 160104. doi:10.1038/sdata.2016.104, 2016.

561 Huang, K., Fu, J. S., Prikhodko, V. Y., Storey, J. M., Romanov, A., Hodson, E. L., Cresko, J.,
562   Morozova, I., Ignatieva, Y., and Cabaniss, J.: Russian anthropogenic black carbon:
563   Emission reconstruction and Arctic black carbon simulation, J Geophys Res-Atmos, 120,
564   11306-11333, doi:10.1002/2015jd023358, 2015.

565 Ikeda, K., Tanimoto, H., Sugita, T., Akiyoshi, H., Kanaya, Y., Zhu, C. M., and Taketani, F.:
566   Tagged tracer simulations of black carbon in the Arctic: transport, source contributions,
567   and budget, Atmospheric Chemistry and Physics, 17, 10515-10533, doi:10.5194/acp-17-
568   10515-2017, 2017.

569 Janssens-Maenhout, G., Crippa, M., Guizzardi, D., Dentener, F., Muntean, M., Pouliot, G.,
570   Keating, T., Zhang, Q., Kurokawa, J., Wankmüller, R., Denier van der Gon, H., Kuenen, J. J.
571   P., Klimont, Z., Frost, G., Darras, S., Koffi, B., and Li, M.: HTAP_v2.2: a mosaic of regional
572   and global emission grid maps for 2008 and 2010 to study hemispheric transport of air
573   pollution, Atmos. Chem. Phys., 15, 11411–11432, doi:10.5194/acp-15-11411-2015, 2015.

574 Keegan, K. M., Albert, M. R., McConnell, J. R., and Baker, I.: Climate change and forest fires
575   synergistically drive widespread melt events of the Greenland Ice Sheet, P Natl Acad Sci
576   USA, 111, 7964-7967, doi:10.1073/pnas.1405397111, 2014.

577 Kipling, Z., Stier, P., Schwarz, J. P., Perring, A. E., Spackman, J. R., Mann, G. W., Johnson, C.
578   E., and Telford, P. J.: Constraints on aerosol processes in climate models from vertically-
579   resolved aircraft observations of black carbon, Atmos. Chem. Phys., 13, 5969–5986,
580   doi:10.5194/acp-13-5969-2013, 2013.

581 Kirchstetter, T. W., Novakov, T., and Hobbs, P. V.: Evidence that the spectral dependence of
582   light absorption by aerosols is affected by organic carbon, J Geophys Res-Atmos, 109,
583   D21208, doi:10.1029/2004jd004999, 2004.

584 Klimont, Z., Kupiainen, K., Heyes, C., Purohit, P., Cofala, J., Rafaj, P., Borken-Kleefeld, J., and
585   Schöpp, W.: Global anthropogenic emissions of particulate matter including black carbon,
586   Atmos. Chem. Phys., 17, 8681–8723, doi:10.5194/acp-17- 8681-2017, 2017.

587 Klonecki, A., Hess, P., Emmons, L., Smith, L., Orlando, J., and Blake, D.: Seasonal changes in
588   the transport of pollutants into the Arctic troposphere-model study, J Geophys Res-
589   Atmos, 108, 8367, doi:10.1029/2002jd002199, 2003.

590   Koch, D., and Hansen, J.: Distant origins of Arctic black carbon: A Goddard Institute for Space

591   Studies ModelE experiment, J Geophys Res-Atmos, 110, D04204,

592   doi:10.1029/2004jd005296, 2005.

593   Koch, D., Schmidt, G. A., and Field, C. V.: Sulfur, sea salt, and radionuclide aerosols in GISS

594   ModelE, J. Geophys. Res., 111, D06206, doi:10.1029/2004jd005550, 2006.

595   Lack, D. A., and Langridge, J. M.: On the attribution of black and brown carbon light

596   absorption using the Angstrom exponent, Atmospheric Chemistry and Physics, 13,

597   10535–10543, doi:10.5194/acp-13-10535-2013, 2013.

598   Law, K. S., and Stohl, A.: Arctic air pollution: Origins and impacts, Science, 315, 1537–1540,

599   doi:10.1126/science.1137695, 2007.

600   Liu, J., Fan, S., Horowitz, L. W., and Levy II, H.: Evaluation of factors controlling long-range

601   transport of black carbon to the Arctic, J. Geophys. Res., 116, D00A14,

602   doi:10.1029/2010JD015145, 2011.

603   Liu, D., Quennehen, B., Darbyshire, E., Allan, J. D., Williams, P. I., Taylor, J. W., Bauguitte, S. J.

604   B., Flynn, M. J., Lowe, D., Gallagher, M. W., Bower, K. N., Choularton, T. W., and Coe, H.:

605   The importance of Asia as a source of black carbon to the European Arctic during

606   springtime 2013, Atmospheric Chemistry and Physics, 15, 11537–11555, doi:10.5194/acp-

607   15-11537-2015, 2015.

608   Ma, P.-L., Rasch, P. J., Wang, H., Zhang, K., Easter, R. C., Tilmes, S., Fast, J. D., Liu, X., Yoon, J.-

609   H., and Lamarque, J.-F.: The role of circulation features on black carbon transport into the

610   Arctic in the Community Atmosphere Model version 5 (CAM5), J. Geophys. Res.-Atmos.,

611   118, 4657–4669, doi:10.1002/jgrd.50411, 2013.

612   McMahon, T. A. and Denison, P. J.: Empirical atmospheric deposition parameters – a survey,

613   Atmos. Environ., 13, 571–585, doi:10.1016/0004-6981(79)90186-0, 1979.

614   Najafi, M. R., Zwiers, F. W., and Gillett, N. P.: Attribution of Arctic temperature change to

615   greenhouse-gas and aerosol influences, Nature Climate Change, 5, 246-249,

616   doi:10.1038/Nclimate2524, 2015.

617   Park, R. J., Jacob, D. J., Palmer, P. I., Clarke, A. D., Weber, R. J., Zondlo, M. A., Eisele, F. L.,

618   Bandy, A. R., Thornton, D. C., Sachse, G. W., and Bond, T. C.: Export efficiency of black

619   carbon aerosol in continental outflow: Global implications, J Geophys Res-Atmos, 110,

620   D11205, doi:10.1029/2004jd005432, 2005.

621 Qi, L., Li, Q. B., Henze, D. K., Tseng, H. L., and He, C. L.: Sources of springtime surface black

622   carbon in the Arctic: an adjoint analysis for April 2008, Atmospheric Chemistry and

623   Physics, 17, 9697–9716, doi:10.5194/acp-17-9697-2017, 2017.

624 Quinn, P. K., Bates, T. S., Baum, E., Doubleday, N., Fiore, A. M., Flanner, M., Fridlind, A.,

625   Garrett, T. J., Koch, D., Menon, S., Shindell, D., Stohl, A., and Warren, S. G.: Short-lived

626   pollutants in the Arctic: their climate impact and possible mitigation strategies,

627   Atmospheric Chemistry and Physics, 8, 1723–1735, doi:10.5194/acp-8-1723-2008, 2008.

628 Ramli, H. M. and Esler, J. G.: Quantitative evaluation of numerical integration schemes for

629   Lagrangian particle dispersion models, Geosci. Model Dev., 9, 2441–2457,

630   doi:10.5194/gmd-9-2441-2016, 2016.

631 Rastigejev, Y., Park, R., Brenner, M., and Jacob, D.: Resolving intercontinental pollution

632   plumes in global models of atmospheric transport, J. Geophys. Res., 115, D02302,

633   doi:10.1029/2009JD012568, 2010.

634 Roiger, A., Thomas, J. L., Schlager, H., Law, K. S., Kim, J., Schafler, A., Weinzierl, B.,

635   Dahloktter, F., Krisch, I., Marelle, L., Minikin, A., Raut, J. C., Reiter, A., Rose, M., Scheibe,

636   M., Stock, P., Baumann, R., Bouapar, I., Clerbaux, C., George, M., Onishi, I., and Flemming,

637   J.: Quantifying emerging local anthropogenic emissions in the Arctic region: The ACCESS

638   aircraft campaign experiment, B. Am. Meteorol. Soc., 96, 441–460, doi:10.1175/Bams-D-

639   13-00169.1, 2015.

640 Sand, M., Berntsen, T. K., von Salzen, K., Flanner, M. G., Langner, J., and Victor, D. G.:

641   Response of Arctic temperature to changes in emissions of short-lived climate forcers,

642   Nature Climate Change, 6, 286-289, doi:10.1038/Nclimate2880, 2016.

643 Schacht, J., Heinold, B., Quaas, J., Backman, J., Cherian, R., Ehrlich, A., Herber, A., Huang, W.

644   T. K., Kondo, Y., Massling, A., Sinha, P. R., Weinzierl, B., Zanatta, M., and Tegen, I.: The

645   importance of the representation of air pollution emissions for the modeled distribution

646   and radiative effects of black carbon in the Arctic, Atmos. Chem. Phys., 19, 11159–11183,

647   doi:10.5194/acp-19-11159-2019, 2019.

648 Schmale, J., Arnold, S. R., Law, K. S., Thorp, T., Anenberg, S., Simpson, W. R., Mao, J., and

649   Pratt, K. A.: Local Arctic Air Pollution: A Neglected but Serious Problem, Earths Future, 6,

650   1385–1412, doi:10.1029/2018ef000952, 2018.

651 Schulz, H., Zanatta, M., Bozem, H., Leaitch, W. R., Herber, A. B., Burkart, J., Willis, M. D.,

652   Kunkel, D., Hoor, P. M., Abbatt, J. P. D., and Gerdes, R.: High Arctic aircraft measurements

653   characterising black carbon vertical variability in spring and summer, Atmospheric

654   Chemistry and Physics, 19, 2361–2384, doi:10.5194/acp-19-2361-2019, 2019.

655   Sharma, S., Leaitch, W. R., Huang, L., Veber, D., Kolonjari, F., Zhang, W., Hanna, S. J.,

656   Bertram, A. K., and Ogren, J. A.: An evaluation of three methods for measuring black

657   carbon in Alert, Canada, Atmospheric Chemistry and Physics, 17, 15225–15243,

658   doi:10.5194/acp-17-15225-2017, 2017.

659   Shaw, G. E.: The arctic haze phenomenon, B Am Meteorol Soc, 76, 2403–2413, 1995.

660   Shen, Z. Y., Ming, Y., Horowitz, L. W., Ramaswamy, V., and Lin, M. Y.: On the seasonality of

661   Arctic black carbon, J. Climate, 30, 4429–4441, doi:10.1175/Jcli-D-16-0580.1, 2017.

662   Shindell, D. T., Chin, M., Dentener, F., Doherty, R. M., Faluvegi, G., Fiore, A. M., Hess, P.,

663   Koch, D. M., MacKenzie, I. A., Sanderson, M. G., Schultz, M. G., Schulz, M., Stevenson, D.

664   S., Teich, H., Textor, C., Wild, O., Bergmann, D. J., Bey, I., Bian, H., Cuvelier, C., Duncan, B.

665   N., Folberth, G., Horowitz, L. W., Jonson, J., Kaminski, J. W., Marmer, E., Park, R., Pringle,

666   K. J., Schroeder, S., Szopa, S., Takemura, T., Zeng, G., Keating, T. J., and Zuber, A.: A multi-

667   model assessment of pollution transport to the Arctic, Atmos. Chem. Phys., 8, 5353-5372,

668   doi:10.5194/acp-8-5353-2008, 2008.

669   Sinha, P. R., Kondo, Y., Koike, M., Ogren, J. A., Jefferson, A., Barrett, T. E., Sheesley, R. J.,

670   Ohata, S., Moteki, N., Coe, H., Liu, D., Irwin, M., Tunved, P., Quinn, P. K., and Zhao, Y.:

671   Evaluation of ground-based black carbon measurements by filter-based photometers at

672   two Arctic sites, J Geophys Res-Atmos, 122, 3544-3572, doi:10.1002/2016jd025843,

673   2017.

674   Stohl, A., Forster, C., Frank, A., Seibert, P., and Wotawa, G.: Technical note: The Lagrangian

675   particle dispersion model FLEXPART version 6.2, Atmos. Chem. Phys., 5, 2461–2474,

676   doi:10.5194/acp-5-2461-2005, 2005.

677   Stohl, A.: Characteristics of atmospheric transport into the Arctic troposphere, J Geophys

678   Res-Atmos, 111, D11306, doi:10.1029/2005jd006888, 2006.

679   Stohl, A., Hittenberger, M., and Wotawa, G.: Validation of the Lagrangian particle dispersion

680   model FLEXPART against large-scale tracer experiment data, Atmos Environ, 32, 4245-

681   4264, doi:10.1016/S1352-2310(98)00184-8, 1998.

682   Stohl, A., Klimont, Z., Eckhardt, S., Kupiainen, K., Shevchenko, V. P., Kopeikin, V. M., and

683   Novigatsky, A. N.: Black carbon in the Arctic: the underestimated role of gas flaring and

684   residential combustion emissions, Atmospheric Chemistry and Physics, 13, 8833-8855,

685   doi:10.5194/acp-13-8833-2013, 2013.

686   Taketani, F., Miyakawa, T., Takashima, H., Komazaki, Y., Pan, X., Kanaya, Y., and Inoue, J.:

687   Shipborne observations of atmospheric black carbon aerosol particles over the Arctic

688   Ocean, Bering Sea, and North Pacific Ocean during September 2014, J Geophys Res-

689   Atmos, 121, 1914-1921, doi:10.1002/2015jd023648, 2016.

690   Tietze, K., Riedi, J., Stohl, A., and Garrett, T. J.: Space-based evaluation of interactions

691   between aerosols and low-level Arctic clouds during the Spring and Summer of 2008,

692   Atmospheric Chemistry and Physics, 11, 3359-3373, doi:10.5194/acp-11-3359-2011,

693   2011.

694   Tilling, R. L., Ridout, A., Shepherd, A., and Wingham, D. J.: Increased Arctic sea ice volume

695   after anomalously low melting in 2013, Nature Geoscience, 8, 643-646,

696   doi:10.1038/Ngeo2489, 2015.

697   Tørseth, K., Aas, W., Breivik, K., Fjæraa, A. M., Fiebig, M., Hjellbrekke, A. G., Lund Myhre, C.,

698   Solberg, S., and Yttri, K. E.: Introduction to the European Monitoring and Evaluation

699   Programme (EMEP) and observed atmospheric composition change during 1972–2009,

700   Atmos. Chem. Phys., 12, 5447–5481, doi:10.5194/acp-12-5447-2012, 2012.

701   Trusel, L. D., Das, S. B., Osman, M. B., Evans, M. J., Smith, B., Fettweis, X., McConnell, J. R.,

702   Noel, B. P. Y., and van den Broeke, M. R.: Nonlinear rise in Greenland runoff in response

703   to post-industrial Arctic warming, Nature, 564, 104-108, doi:10.1038/s41586-018-0752-4,

704   2018.

705   van der Werf, G. R., Randerson, J. T., Giglio, L., Collatz, G. J., Mu, M., Kasibhatla, P. S.,

706   Morton, D. C., DeFries, R. S., Jin, Y., and van Leeuwen, T. T.: Global fire emissions and the

707   contribution of deforestation, savanna, forest, agricultural, and peat fires (1997–2009),

708   Atmospheric Chemistry and Physics, 10, 11707-11735, doi:10.5194/acp-10-11707-2010,

709   2010.

710   Veira, A., Lasslop, G., and Kloster, S.: Wildfires in a warmer climate: Emission fluxes,

711   emission heights, and black carbon concentrations in 2090-2099, J Geophys Res-Atmos,

712   121, 3195-3223, doi:10.1002/2015jd024142, 2016.

713   Wang, H., Rasch, P. J., Easter, R. C., Singh, B., Zhang, R., Ma, P. L., Qian, Y., and Beagley, N.:

714   Using an explicit emission tag- ging method in global modeling of source-receptor

relationships for black carbon in the Arctic: Variations, Sources and Trans- port pathways, J. Geophys. Res.-Atmos., 119, 12888–12909, doi:10.1002/2014JD022297, 2014.

Wang, Q., Jacob, D. J., Fisher, J. A., Mao, J., Leibensperger, E. M., Carouge, C. C., Le Sager, P., Kondo, Y., Jimenez, J. L., Cubison, M. J., and Doherty, S. J.: Sources of carbonaceous aerosols and deposited black carbon in the Arctic in winter-spring: implications for radiative forcing, Atmos. Chem. Phys., 11, 12453– 12473, doi:10.5194/acp-11-12453-2011, 2011.

Wang, Q., Jacob, D. J., Spackman, J. R., Perring, A. E., Schwarz, J. P., Moteki, N., Marais, E. A., Ge, C., Wang, J., and Barrett, S. R. H.: Global budget and radiative forcing of black carbon aerosol: constraints from pole-to-pole (HIPPO) observations across the Pacific, J. Geophys. Res. Atmos., 119, 195–206, doi:10.1002/2013JD020824, 2014.

Winiger, P., Andersson, A., Eckhardt, S., Stohl, A., and Gustafsson, O.: The sources of atmospheric black carbon at a European gateway to the Arctic, Nat Commun, 7, 12776, doi:10.1038/ncomms12776, 2016.

Winiger, P., Barrett, T. E., Sheesley, R. J., Huang, L., Sharma, S., Barrie, L. A., Yttri, K. E., Evangeliou, N., Eckhardt, S., Stohl, A., Klimont, Z., Heyes, C., Semiletov, I. P., Dudarev, O. V., Charkin, A., Shakhova, N., Holmstrand, H., Andersson, A., and Gustafsson, O.: Source apportionment of circum-Arctic atmospheric black carbon from isotopes and modeling, Sci Adv, 5, eaau8052, doi:10.1126/sciadv.aau8052, 2019.

Xu, J. W., Martin, R. V., Morrow, A., Sharma, S., Huang, L., Leaitch, W. R., Burkart, J., Schulz, H., Zanatta, M., Willis, M. D., Henze, D. K., Lee, C. J., Herber, A. B., and Abbatt, J. P. D.: Source attribution of Arctic black carbon constrained by aircraft and surface measurements, Atmospheric Chemistry and Physics, 17, 11971-11989, doi:10.5194/acp-17-11971-2017, 2017.

Yang, Y., Wang, H., Smith, S. J., Easter, R. C., and Rasch, P. J.: Sulfate aerosol in the Arctic: Source attribution and radiative forcing, J. Geophys. Res. Atmos., 123, 1899–1918, doi:10.1002/2017JD027298, 2018.

Yang, Y., Smith, S. J., Wang, H., Mills, C. M., and Rasch, P. J.: Variability, timescales, and nonlinearity in climate responses to black carbon emissions, Atmospheric Chemistry and Physics, 19, 2405–2420, doi:10.5194/acp-19-2405-2019, 2019.

Yu, K., Keller, C. A., Jacob, D. J., Molod, A. M., Eastham, S. D., and Long, M. S.: Errors and improvements in the use of archived meteorological data for chemical transport

747   modeling: an analysis using GEOS-Chem v11-01 driven by GEOS-5 meteorology, Geosci

748   Model Dev, 11, 305-319, doi:10.5194/gmd-11-305-2018, 2018.

749   Zhu, C., Kobayashi, H., Kanaya, Y., and Saito, M.: Size-dependent validation of MODIS

750   MCD64A1 burned area over six vegetation types in boreal Eurasia: Large underestimation

751   in croplands, Scientific reports, 7, 4181, doi:10.1038/s41598-017-03739-0, 2017.

Table 1. Comparison of BC source contributions in the Arctic surface

Model and versions	Model type	Wet-deposition	Grid resolution	Meteorology	Emissions	Domain/Sites	Year/season	Major source regions/sectors	Reference
Flexpart-WRF 6.2	Lagrangian	Stohl et al. (2005)	unspecified	WRF forcast	ECLIPSE, FINN	continental Norway and Svalbard	spring 2013	Asian anthropogenic	Liu et al. (2015)
Flexpart 6.2	Lagrangian	Stohl et al. (2005)	1° × 1°	ECMWF operational	Unspecified (BC sensitivities were calculated)	Alert, Barrow, Zeppelin	1989-2009	Northern Eurasia	Hirdman et al. (2010)
Flexpart 6.2	Lagrangian	Stohl et al. (2005)	1° × 1°	ECMWF operational	ECLIPSE4(GAINS), GFED3	Arctic (north of 66°N)	2008-2010	Flaring (42%), residential (>20%)	Stohl et al. (2013)
Flexpart 9.2	Lagrangian	Stohl et al. (2005)	1° × 1°	ECMWF operational	ECLIPSE5(GAINS), GFED4.1	Arctic (north of 66.7°N)	2011-2015	Residential and open burning (39%)	Winiger et al. (2019)
Flexpart 10.1	Lagrangian	Grythe et al. (2017)	1° × 1°	ECMWF operational	HTAP2, GFED3, Huang et al. (2015) for Russia flaring	Arctic (north of 66°N)	2010	Flaring (36%), open burning (18%), residential (15%), others (31%)	Current study
GEOS-Chem 9.02	CTM	Wang et al. (2011)	2° × 2.5°	GEOS-5	HTAP2, GFED3, Huang et al. (2015) for Russia flaring	Arctic (north of 66°N)	2007-2011	Russia (62%)	Ikeda et al. (2017)
GEOS-Chem	CTM	Wang et al. (2011)	2° × 2.5°	GEOS-5	Bond et al. (2004), Zhang et al. (2009), GFED3	Alert, Barrow, Zeppelin	April 2008	Asian anthropogenic (35–45%), Siberian biomass burning (46–64%)	Qi et al. (2017)
GEOS-Chem	CTM	Wang et al. (2011)	2° × 2.5°	GEOS-5	Bond et al. (2007), FLAMBE	North America Arctic	April 2008	Open fire (50%)	Wang et al. (2011)

GEOS-Chem10.01	CTM	Wang et al. (2011)	2° × 2.5°	GEOS-5	HTAP2, ECLIPSE5, GFED4	Alert, Barrow, Zeppelin, Arctic (north of 66.5°N)	2009-2011	N-Asian anthropogenic (40–45%) in winter-spring	Xu et al. (2017)
GISS ModelE	GCM	Koch et al. (2006)	4° × 5°	Internal	Bond et al. (2004), Cooke and Wilson (1996)	Arctic (north of ~60°N)	Annual general	South Asia	Koch and Hansen (2005)

752
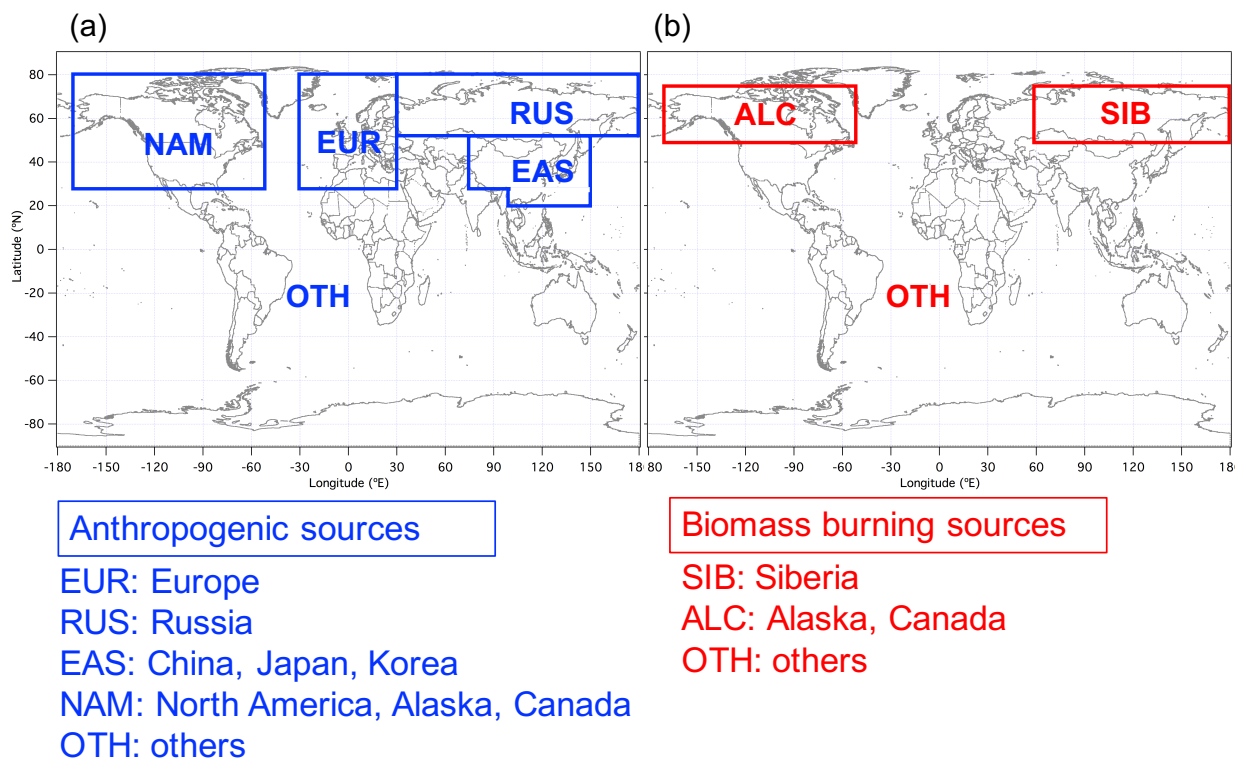
753

754 Figure 1. Regional separation for quantification of BC in the Arctic from (a) anthropogenic and

755 (b) open biomass burning sources.

756
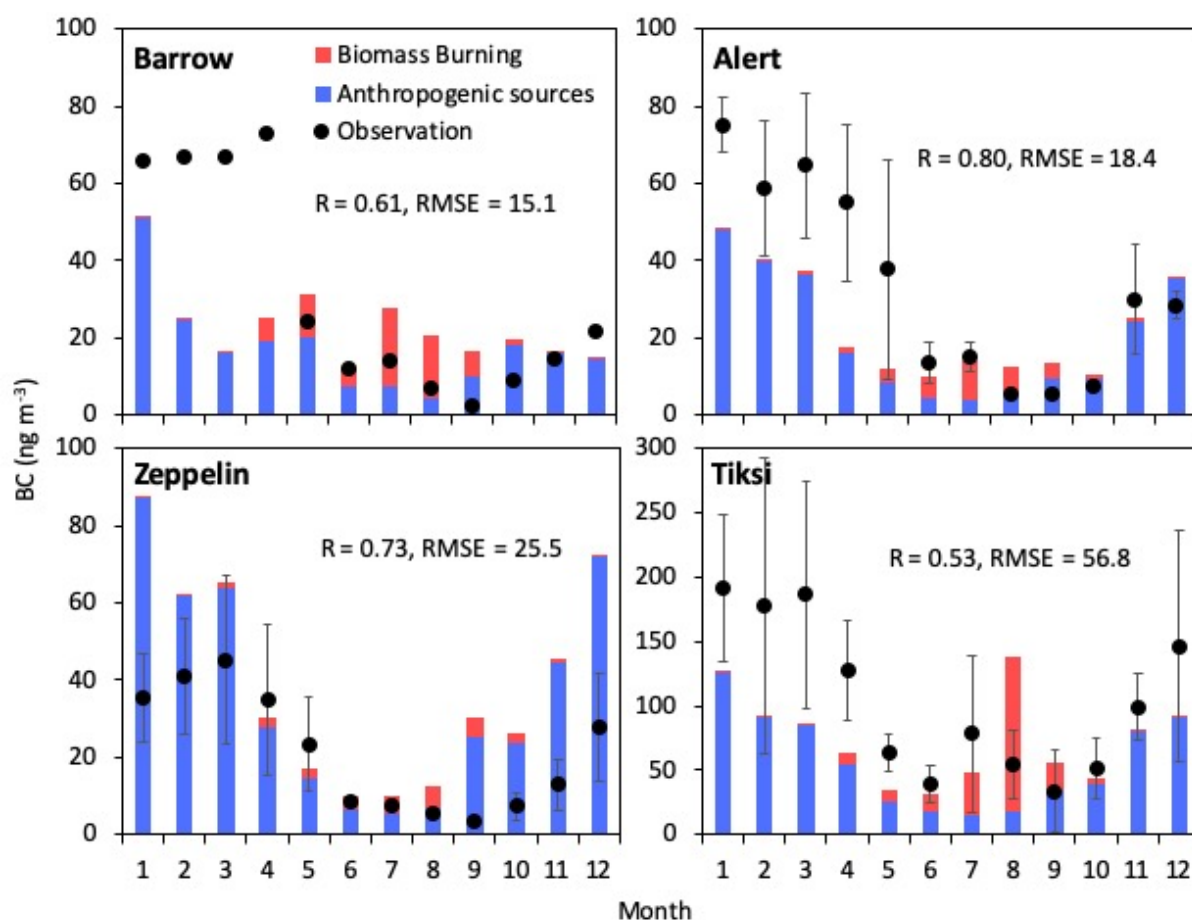
Figure 2. Observed (filled circles) and modeled (bars) seasonal variations in BC mass concentrations at Arctic sites. Contributions from anthropogenic sources (blue) and open biomass burning (red) in each month are shown. Monthly averages of observed (filled circles) and simulated (bars) BC were conducted for 2007–2011 at Alert, Canada (62.3° W, 82.5° N), and Zeppelin, Norway (11.9° E, 78.9° N), for 2009 at Barrow, USA (156.6° W, 71.3° N), and for 2010–2014 at Tiksi, Russia (128.9° E, 71.6° N). *R* and RMSE indicate correlation coefficient and root-mean-square error (ng m^{-3}), respectively.
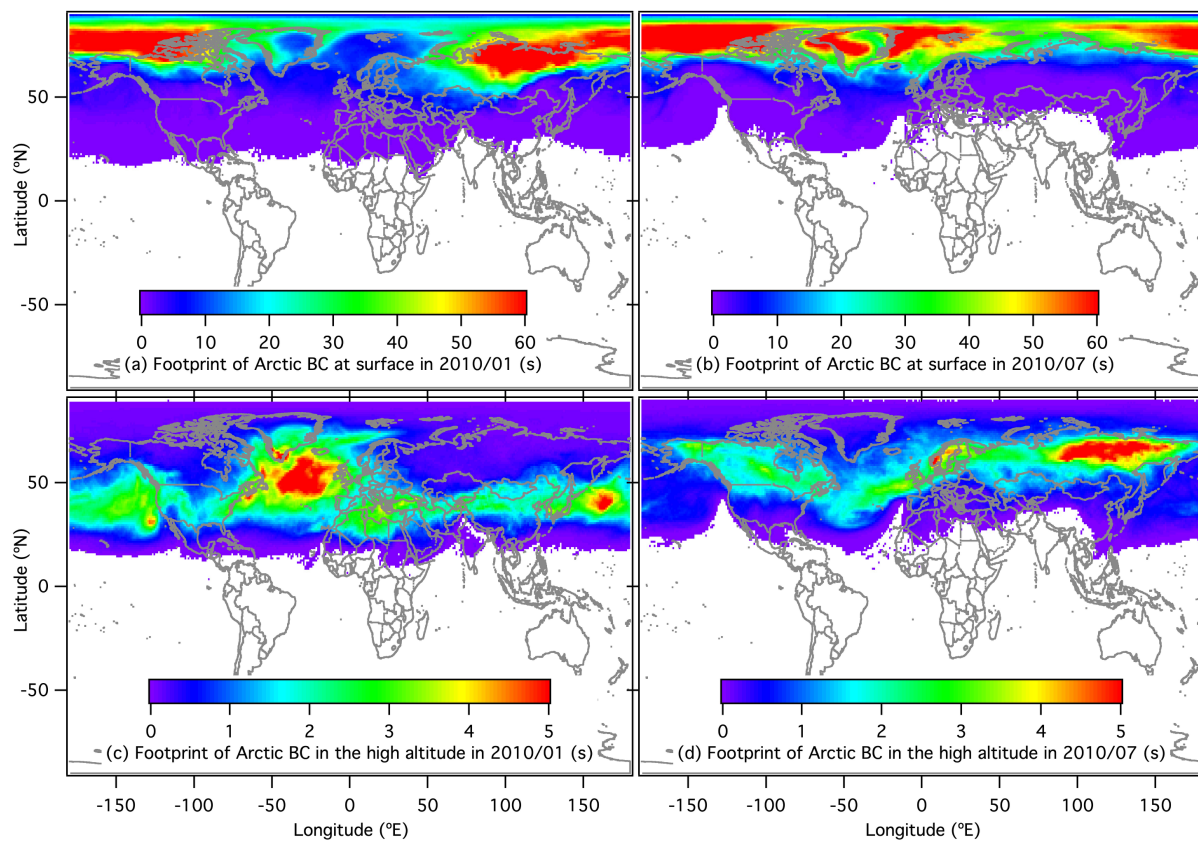
Figure 3. Footprints of Arctic BC shown as retention time(s) of (a) BC at surface (0–500 m) in January 2010, (b) BC at surface in July 2010, (c) BC at high altitudes (4750–5250 m) in January 2010, and (d) BC at high altitudes in July 2010.
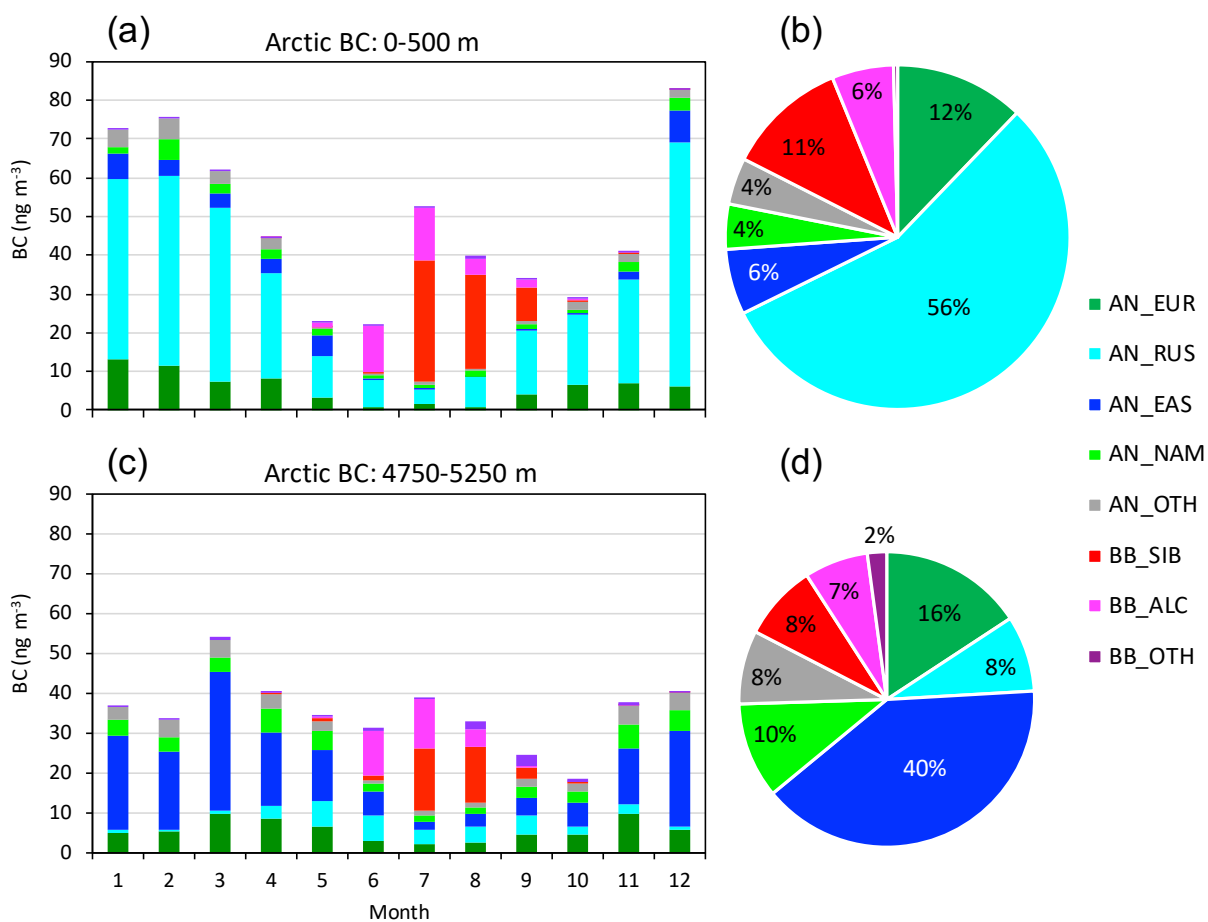
Figure 4. Contributions of anthropogenic sources (prefixed "AN_" in the legend) and open biomass burning ("BB_") from each region to (a) seasonal variations in Arctic surface BC, (b) annual mean Arctic surface BC, (c) seasonal variations in Arctic BC at high altitudes, and (d) annual mean of Arctic BC at high altitudes.
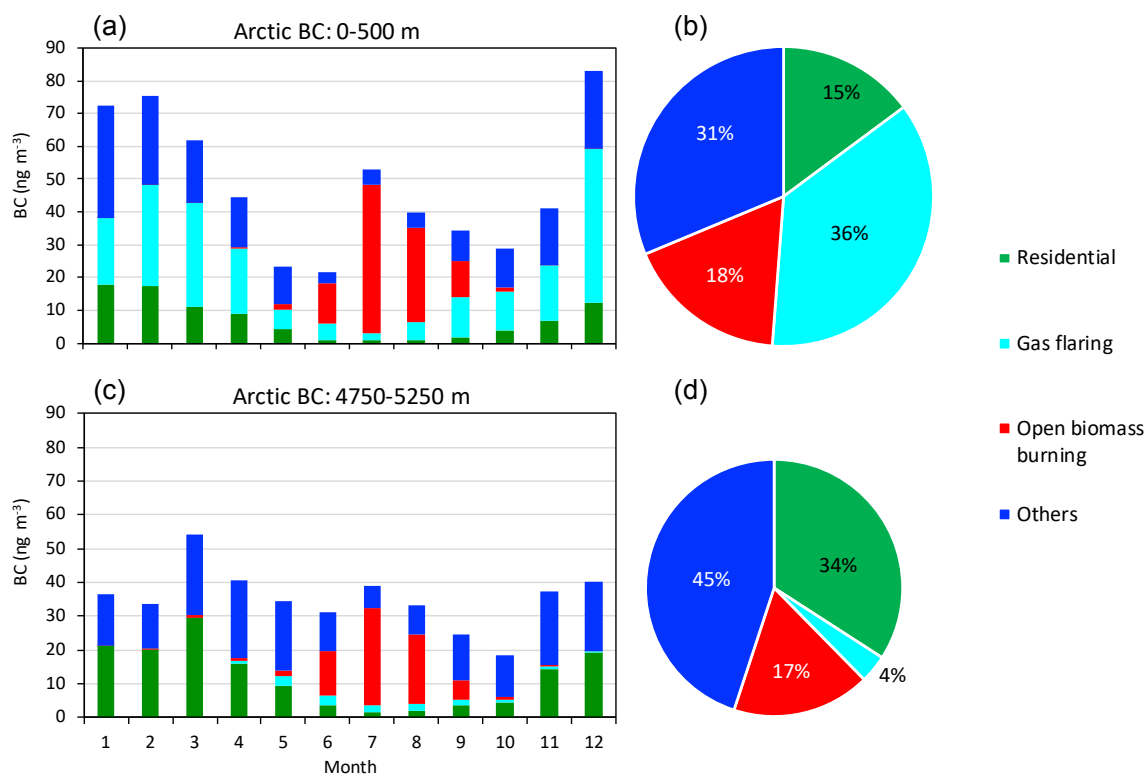
777

778 Figure 5. Sectorial contributions from residential combustion (including fossil fuel and biofuel

779 combustions), gas flaring, open biomass burning and others (energy other than gas flaring,

780 industry and transport) to (a) seasonal variations in Arctic surface BC, (b) annual mean Arctic

781 surface BC, (c) seasonal variations in Arctic BC at high altitudes, and (d) annual mean of Arctic

782 BC at high altitudes.

783
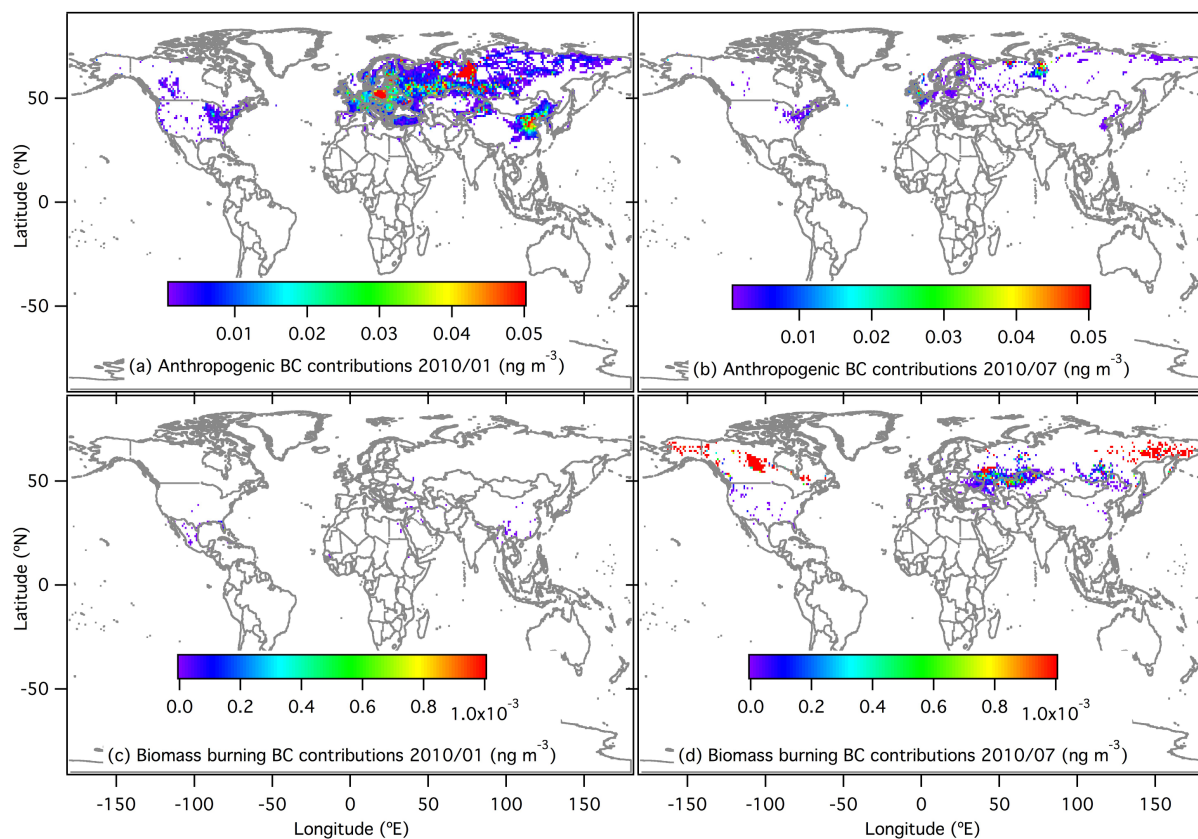
784

785 Figure 6. Spatial distributions of contributions to Arctic BC at surface for (a) anthropogenic

786 contributions in January 2010, (b) anthropogenic contributions in July 2010, (c) open biomass

787 burning contributions in January 2010, and (d) open biomass burning contributions in July

788 2010.

789
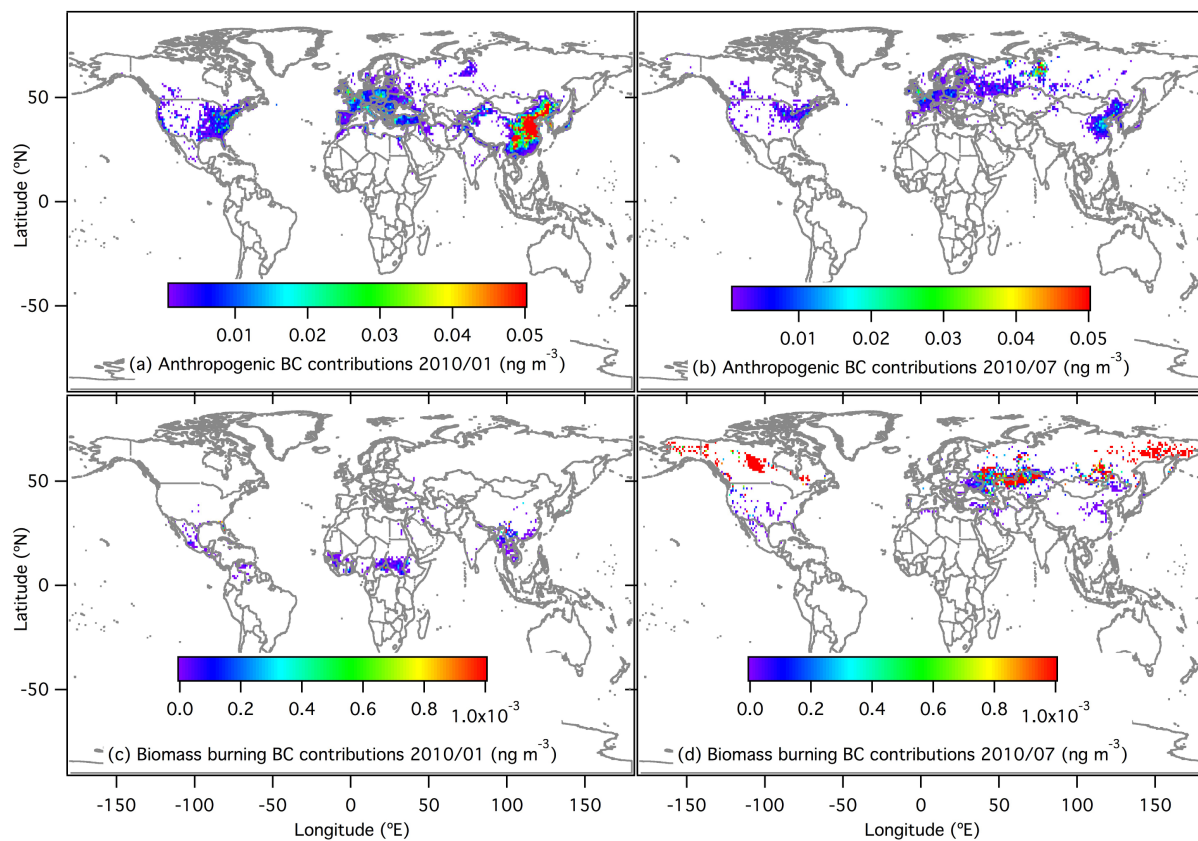
Figure 7. Spatial distributions of contributions to Arctic BC at high altitudes for (a) anthropogenic contributions in January 2010, (b) anthropogenic contributions in July 2010, (c) open biomass burning contributions in January 2010, and (d) open biomass burning contributions in July 2010.